Drug Metab Drug Interact 2011;26(3):91–104 © 2011 by Walter de Gruyter • Berlin • Boston. DOI 10.1515/DMDI.2011.014

Review

Theoretical prediction of drug-receptor interactions

Vladimir Frecer*

Department of Physical Chemistry of Drugs, Faculty of Pharmacy, Comenius University, and Cancer Research Institute, Slovak Academy of Sciences, Bratislava, Slovakia

Abstract

The crucial event in the pharmacological action of drugs is the interaction between a drug molecule and its receptor. Molecular recognition and binding affinity of a drug is driven by a flexible steric fit and a molecular field match between two complementary molecular surfaces of the receptor and the approaching ligand. Rational drug design methods, which attempt to predict the free energy change resulting from ligand binding, rely on a detailed knowledge of the physical forces that govern the drug-receptor interactions in several populated configurations of the intermolecular complex. The overall strength of the interaction is determined by the fine balance between the forces contributed by the individual chemical function groups of the two entities and the physiological medium. This paper recounts some basic information about the description of molecular structures and highlights the methods and approximations commonly used to calculate the binding affinity of a drug to its receptor.

Keywords: binding affinity; docking; drug-receptor interactions; intermolecular forces; molecular modeling and simulations; quantum chemistry; scoring functions

Introduction

Most drugs, typically small organic molecules, achieve their desired therapeutic effect by interacting selectively with target biopolymers (drug receptors), which play an important role in physiologic or pathophysiologic processes within organisms.[1] The sites of drug action include proteins, nucleic acids, lipids and saccharides; however, the most common targets are proteins, such as enzymes, membrane-bound receptors, ion channels, antibodies and structural proteins. The binding of drugs to the receptor's active sites causes changes in the processes controlled by these receptors (or enzymes) by preventing the binding of endogenous ligands (substrates) to the receptor binding pockets. The activation or inhibition of the cellular receptors induced by the drug binding may lead to a cumulative dose-dependent response effect that can be observed at a tissue (organ) or organism level (1). In a model system:

$$\underset{\text{Potency}}{D+R \underset{k_{off}}{\overset{k_{on}}{\rightleftarrows}} DR} \left(\underset{k_b}{\overset{k_a}{\rightleftarrows}} DR^* \right)_{\text{Efficacy}} \quad K_d = \frac{k_{off}}{k_{on}}$$

$$\text{Response fraction} = \frac{[DR]}{[R_0]} = \frac{[D]}{[D]+K_d} \qquad [1]$$

where [D] is the free drug concentration, $[R_0]=[R]+[DR]$ is total concentration of free and occupied receptors, k_{on} and k_{off} are rate constants, and K_d is the equilibrium dissociation constant of the reversible drug-receptor complex or DR (DR* is activated complex).[2]

Thus, besides drug concentration, the observed pharmacodynamic effect of a drug[3] (assuming fast receptor activation, $k_a >> k_b$) is closely related to drug-receptor binding potency, K_d, which is an intrinsic property for each DR complex.

The dissociation constant depends (at human body temperature, T) on the Gibbs free energy (ΔG_{bin}) of drug-receptor binding: $\ln K_d = \Delta G_{bin}/RT$ (where R is the gas constant). The ΔG_{bin}, which in reversible complexes is proportional to the sum of noncovalent drug-receptor interactions averaged over an ensemble of the most probable configurations of the DR complex as well as solvent reorganization upon the drug binding, defines the observed affinity and specificity of receptor binding for the ligand.[4] The overall strength of the nonbonding interactions between the receptor and the

[1]Other drugs exist that act by nonreceptor-mediated mechanisms.

*Corresponding author: Vladimir Frecer, Department of Physical Chemistry of Drugs, Faculty of Pharmacy, Comenius University, Odbojarov 10, Bratislava 83232, Slovakia
Phone: +421 2 5011 7281, Fax: +421 2 5011 7100,
E-mail: frecer@fpharm.uniba.sk

Received June 7, 2011; accepted August 11, 2011

[2]Although relatively rare, covalent interaction between drug and receptor lead to essentially irreversible DRs. Drugs that modify their target receptors (often enzymes) through this mechanism (suicide inhibitors) will not be considered here.

[3]Agonists produce the same or greater effect than the natural substrate or effector molecule; whereas antagonists inhibit the effect of the natural ligand. Inverse antagonists create an effect that appears opposite to that of the agonist.

[4]For the purpose of discussion, the terms drug and ligand; target, receptor, enzyme and biomacromolecule will be used interchangeably in this paper.

drug is defined by the matching of the molecular fields of the two complementary molecular surfaces. The binding affinity is determined by the fine balance between the forces contributed by the individual chemical function groups of the two entities and the effect of the solvent and salt ions. These nonbonding interactions play a central role in pharmacology and a major part of life sciences, as it is known that the three-dimensional (3D) structure and function of biomacromolecules, macromolecular associations, membrane formation, ligand-receptor binding and other biochemical events are dominated by weak noncovalent intermolecular interactions, such as hydrogen bonding, salt bridges, charge transfer, π-π stacking, aromatic-polar and dispersion interactions as well as solvation (2).

This review focuses on molecular details of drug-receptor interactions of tight-binding ligands and their description by means of quantum chemistry, molecular simulations and modeling. An accurate prediction of the binding affinity of a drug candidate to its receptor is central to most of the computer-assisted drug design approaches.

Structure of drug-receptor complexes

A 3D structure of receptors and DRs at the atomic level of resolution, which is a required input for computational studies on ligand-receptor interactions, can be obtained from X-ray diffraction analyses of crystal structures, nuclear magnetic resonance (NMR) spectroscopic measurements on the DRs in solution or from protein homology modeling and ligand docking (3–6).

An individual protein molecule in solution constantly fluctuates among various conformational states whereas structure determination techniques provide a time and ensemble-averaged picture of a protein's 3D structure. The structural dynamics of a protein receptor is essential for the process of ligand-receptor binding, as in many cases only a conformational change in the receptor permits the accommodation of a ligand (7). The role of conformational changes in ligand binding was rationalized by the mechanisms of induced-fit (8) and pre-existing equilibrium dynamics (9). In the former, the binding of a ligand induces the necessary conformational change, while in the latter the ligand binds to a distinct receptor conformation already present in the set of conformational states accessed by the equilibrium dynamics.

Intermolecular interactions

Quantum mechanical description of molecules

The interactions of atoms in molecules and between molecules are driven purely by electromagnetic forces (see Table 1), similar to all chemical and biological processes.

The interactions in biological media must be sufficiently strong to ensure specific binding between molecules in the heterogeneous environment, but these interactions should not be too strong 'to avoid formation of crystalline species within the cell' (10). The electromagnetic forces acting on the level of atoms and molecules can be described by the time-independent Schrödinger equation:

$$\hat{H}\Psi(\mathbf{r}_1, \ldots, \mathbf{r}_n, \mathbf{R}_1, \ldots, \mathbf{R}_N) = E\Psi(\mathbf{r}_1, \ldots, \mathbf{r}_n, \mathbf{R}_1, \ldots, \mathbf{R}_N) \quad [2]$$

for a system composed of n electrons (1,..., i, j,..., n) and N atomic nuclei (1,..., A, B,..., N), for which $\Psi(\mathbf{r}_1,..., \mathbf{r}_n, \mathbf{R}_1,..., \mathbf{R}_N)$ represents the wave function dependent on the position vectors of the moving electrons ($\mathbf{r}_i$) and nuclei ($\mathbf{R}_A$) that characterize their motion. In Eq. [2], E is the total energy of the system and $\hat{H}$ denotes the Hamiltonian operator (11):

$$\hat{H} = -\frac{\hbar^2}{2}\sum_A \frac{1}{M_A}\nabla_A^2 - \frac{\hbar^2}{2m_e}\sum_i \nabla_i^2 - \sum_i \sum_A \frac{Z_A e^2}{r_{iA}} + \sum_i \sum_{<j} \frac{e^2}{r_{ij}} + \sum_A \sum_{<B} \frac{Z_A Z_B e^2}{R_{AB}} = T_N + T_e + V_{eN} + V_{ee} + V_{NN}$$

$$f_{x_A} = -\frac{\partial E}{\partial x_A} = -\left\langle \Psi \left| \frac{\partial \hat{H}}{\partial x_A} \right| \Psi \right\rangle \quad [3]$$

where T_N and T_e are the kinetic energies of nuclei and electrons, V_{eN} is the potential energy of electrostatic attraction between electrons and nuclei, and V_{ee} and V_{NN} represent the potential energies of electrostatic repulsion between electrons and between nuclei, respectively. The summation indices i, j and A, B extend over electrons and nuclei, m and M are masses, Z is the nuclear charge number, and r and R are the appropriate distances.

Solution of the eigenvalue problem – the Schrödinger equation [2], leads to stationary states of wave function Ψ_k and corresponding discrete values of the total energy of the system ε_k. According to the Born interpretation, the distribution of electron density in the molecule is equal to the square of the wave function $\Psi\Psi^*$. The Hellmann-Feynman theorem relates the

Table 1 Fundamental forces of nature.

Force	Relative strength	Range	Interaction	Field of science
Strong	~10^3	10^{-15} m	Atomic nuclei	Nuclear physics
Electromagnetic[a]	1	Infinite	Atoms, molecules, molecular complexes, solids	Molecular physics, chemistry, biology, electronics, etc.
Weak	~10^{-2}	10^{-17} m	Atomic nuclei	Nuclear physics
Gravitation	~10^{-36}	Infinite	Macroscopic bodies	Physics, astronomy

[a]Contacts between molecules in a supermolecular complex occur at distances of approximately 10^{-10} m (1Å), therefore the only relevant force driving the molecular association is the electromagnetic one.

intramolecular forces acting on atoms $\mathbf{F}_A=\left(f_{x_A}, f_{y_A}, f_{z_A}\right)$ to the expectation value of the derivative of the Hamiltonian with respect to the nuclear coordinates (shown in Dirac notation). The forces are useful for finding the equilibrium molecular structures (12).

The Schrödinger equation cannot be solved exactly for systems that contain three or more particles (e.g., a He atom), however, it is possible to solve this equation exactly for the simplest molecular species H_2^+, when the motion of the electrons is decoupled from the motion of the nuclei in accordance with the Born-Oppenheimer approximation:

$$\Psi(\mathbf{r}_1,\cdots,\mathbf{r}_n,\mathbf{R}_1,\cdots,\mathbf{R}_N)=\Psi_R^e(\mathbf{r}_1,\cdots,\mathbf{r}_n)\Psi^N(\mathbf{R}_1,\cdots,\mathbf{R}_N)$$

$$\hat{H}^e\Psi_R^e(\mathbf{r}_1,\cdots,\mathbf{r}_n)=E_R^e\Psi_R^e(\mathbf{r}_1,\cdots,\mathbf{r}_n)$$

$$\hat{H}^e=T_e+V_{eN}+V_{ee}$$

$$E=E_R^e(\mathbf{r}_1,\ldots,\mathbf{r}_n)+E_R^N=\langle\Psi_R^e(\mathbf{r}_1,\ldots,\mathbf{r}_n)|\hat{H}^e|\Psi_R^e(\mathbf{r}_1,\ldots,\mathbf{r}_n)\rangle+\sum_A\sum_B\frac{Z_AZ_Be^2}{R_{AB}} \quad [4]$$

If this approximation is used for polyelectronic systems, such as molecules, we solve the Schrödinger equation for the motion of the electrons in the electrostatic field of fixed nuclei for each molecular configuration, taking into account that the light and fast electrons ($M_A \geq 1836\ m_e$) can adjust almost instantaneously to any change in the positions of the nuclei.

The term $\langle\Psi_R^e(\mathbf{r}_1,\cdots,\mathbf{r}_n)|\hat{H}^e|\Psi_R^e(\mathbf{r}_1,\cdots,\mathbf{r}_n)\rangle$ in Eq. [4] represents the solution of the Schrödinger equation for a normalized wave function in the Dirac notation (12). Even with this simplification introduced, the electronic Schrödinger equation for molecules can only be solved in an approximate way.

Molecular orbital (MO) method assumes that the exact antisymmetric wave function of a polyelectronic molecule (that obeys the Pauli principle) can be replaced by a Slater determinant composed of one-electron functions – spin orbitals ($\Phi_i\eta_s$, where η_s is the spin function), which are expressed as a linear combination of atomic orbitals (χ_i): $\Phi_i=\sum_\mu c_{\mu i}\chi_i$. The approximate solution of the Schrödinger equation for molecular orbitals is done in an iterative way using the Hartree-Fock (HF) self-consistent field (SCF) approach (13, 14) by applying Roothaan and Hall equations to a basis set of atomic orbitals (15, 16). As a result, one obtains the molecular wave function composed of molecular orbitals and the distribution of electron density around the nuclei as well as the orbital energies and the total energy of the molecule as a function of nuclear coordinates (molecular conformation).[5]

Two categories of solutions of the Roothaan-Hall equations exist: the ab initio method, which requires no further approximations (17, 18); and the semi-empirical methods, which use additional approximations and adjustable parameters fitted to experimental data, such as heats of formation, dipole moments, ionization potentials, and molecular geometries (19). The precision of ab initio SCF quantum chemical calculations depends on the type and size of the set of atomic orbitals used, while the accuracy increases when the size of the basis set approaches the complete basis set limit. Faster to compute semi-empirical SCF methods, such as CNDO, MINDO, MNDO, AM1, PM3, SAM1, RM1 or PM6 (20–23) can be applied to larger systems for which the use of ab initio method is prohibitive.

In the Hartree-Fock SCF method, electrons are assumed to be moving in an averaged potential of all other electrons and the approach neglects a part of the mutual correlation of the electron motions. The missing component of the total energy – the correlation energy, defined as the difference between exact (experimental) energy and Hartree-Fock limit obtained for calculation using the complete basis set – is incorporated into molecular orbital calculations by various approaches (24).

The configuration interaction (CI) method, in which excited states are included in the description of the molecular electronic state, expresses the overall wave function as a linear combination of the ground state and excited state wave functions (Slater determinants): $\Psi=c_0\Psi_0+c_1\Psi_1+c_2\Psi_2+\ldots$ (25).

In the Møller and Plesset (MP) many body perturbation theory (26), however, the true Hamiltonian of a molecule is written out as sum of zero-order Hartree-Fock Hamiltonian $\hat{H}_0$, for which molecular orbitals can be obtained, and a small perturbation $\hat{U}$: $\hat{H}=\hat{H}_0+\lambda\hat{U}$.

The eigen-function and eigen-values of energy can be expressed as power series of the expansion parameter λ, which allows derivation of terms for the n-th order energy corrections, as well as higher-order wave function composed of linear combinations of Slater determinants including electron excitations.

Another approach for the estimation of correlation energy, the coupled clusters (CC) method (25), defines the correlated wave function as an exponential series of 'clusters' of SCF eigen-functions containing single, double and triple electron excitations. The coupled cluster with single and double and perturbative triple excitations – CCSD(T) – calculations in extended basis sets represent perhaps the most accurate computational chemistry benchmark data on molecular energies (approaching chemical accuracy, i.e., error in $\Delta\bar{E}_{tot}<4\ kJ\ mol^{-1}$), which can currently be obtained for small-to-medium size organic molecules (27).

The density functional theory (DFT) approach to the electronic structure of atoms and molecules represents a faster-to-calculate alternative to ab initio post-SCF methods (28). It is based on a theorem of Hohenberg and Kohn (29), which states that all ground-state properties of a system are functions of the electron density: $\rho(\mathbf{r})=\sum_i^{N_{occ}}\left|\Phi_i(\mathbf{r}_i)\right|^2$, including the total electronic energy. The electron density and electronic energy are obtained by iteratively solving Kohn-Sham one-electron equations in a basis set of orbitals:

$$\hat{H}_{KS}\Phi_i(\mathbf{r}_i)=\varepsilon_i\Phi_i(\mathbf{r}_i)$$

$$\hat{H}_{KS}=-\frac{\hbar^2}{2m_e}\nabla_i^2+\sum_A\frac{Z_Ae^2}{r_{iA}}+\int\frac{\rho(\mathbf{r}_j)e^2}{r_{ij}}d\mathbf{r}_j+V_{XC}(\mathbf{r}_i)=T_e+V_{eN}+V_{ee}+V_{XC} \quad [5]$$

[5]Other physicochemical properties of the molecule can also be obtained from the molecular wave function.

where the V_{XC} term is the exchange-correlation functional, which can be expressed as a local density approximation of the uniform electron gas model or by various other more sophisticated approximate functionals (30–32). The comparison of physicochemical molecular properties computed by the DFT method to CI, CC or MP calculations showed that the fast DFT calculations are superior to HF calculations and are comparable to the results obtained from the more expensive ab initio CC method (33).

The treatment of large, condensed phase systems (e.g., proteins in aqueous solution) entirely by ab initio or DFT methods is extremely expensive computationally. However, the theoretical prediction of molecular structure, conformational energies and thermochemical properties of small organic drug-like molecules with a sufficient precision is now a standard practice complementing the experimental studies (18, 27).

Biological medium

Intermolecular interactions in a biological environment, such as drug-receptor binding, occur in complex heterogeneous surroundings (including, for example, the proximity of macromolecular structures of various biopolymers, phospholipid membranes, water, salt ions, endogenous substances, and others). These affect the course of biochemical processes via their steric effects and molecular field interference. The effect of ubiquitous water (condensed medium) in particular affects the electronic structure and preferred conformations of dissolved solutes, and influences the forces between the interacting particles (34, 35).

Several computational approaches were developed to model the effect of the solvent. The explicit solvent model adds one or more solvation layers of discrete solvent molecules around the solute and treats the whole system as a 'supermolecule' (36). The implicit models, in contrast, replace the configuration of discrete solvent molecules with a homogeneous medium characterized by a macroscopic property: dielectric constant – reaction field model (37–39), Poisson-Boltzmann model (40), generalized Born model (41) – or polarizability density – Langevin dipoles (42). The reaction field model can be incorporated into quantum chemical calculations by considering the reaction field to be a perturbation of the gas-phase Hamiltonian ($\hat{H}_0$) (37):

$$\hat{H}=\hat{H}_0+\hat{H}_{RF} \qquad \hat{H}_{RF}=\int_s \frac{\sigma(\mathbf{s})}{r}\,d\mathbf{s} \qquad \sigma(\mathbf{s})=\frac{\varepsilon-1}{4\pi\varepsilon}\left[\frac{\partial(V_\rho+V_\sigma)}{\partial n}\right]_{n-}$$

$$\Delta G_{sol}^{els}=<\psi\left|\hat{H}_0+\hat{H}_{RF}\right|\psi>-<\psi_0\left|\hat{H}_0\right|\psi_0>-\tfrac{1}{2}<\psi\left|\hat{H}_{RF}\right|\psi> \qquad [6]$$

where the reaction field Hamiltonian $\hat{H}_{RF}$ is expressed as the electrostatic potential of a charge density $\sigma(\mathbf{s})$, induced on the molecular cavity surface by the solute charge distribution $\rho(\mathbf{r})$ and by itself, and is computed iteratively (37).

In continuum models of solvation, besides the electrostatic component, it is convenient to include the dispersion-repulsion $\left(G_{sol}^{d\text{-}r}\right)$ and cavitation $\left(G_{sol}^{cav}\right)$ terms (34):

$$G_{sol}=G_{sol}^{els}+G_{sol}^{d-r}+G_{sol}^{cav} \qquad [7]$$

Molecular conformation

The total energy of a molecule obtained from a quantum chemical calculation is a parametric function of N nuclear positions (3N Cartesian coordinates or 3N-6 internal coordinates), which define the molecular geometry or conformation and forms a complex hypersurface with energy minima and maxima (11). Molecules are in constant thermal motion and undergo internal rotations and conformational changes. The local minima or global minimum on the energy hypersurface (stationary states) correspond to stable conformations, which are most frequently accessed during the dynamic equilibrium in a given solvent. The global energy minimum – the most stable (reference) configuration – is of special interest to chemists and pharmacologists, therefore, the identification of the relevant molecular geometry of a studied molecule by conformational searching and energy minimization (geometry optimization) is a common task.

Conformational searching on the energy hypersurface can be done in a systematic or stochastic manner (Monte Carlo, molecular dynamics, simulated annealing) and several algorithms exist for geometry optimization (simplex method, steepest descent, conjugate gradient, Newton-Raphson, etc.) (11, 25, 43, 44). Molecular conformation, energy, wave function and related physicochemical properties of the global minimum configuration serve for the calculation of reaction heats, binding affinities and other physicochemical properties of molecules.

Molecular associations

The formation of van der Waals (noncovalent) intermolecular associations, such as drug-receptor complexes, is connected with bonding energies below 60–80 kJ·mol^{-1} and bonding distances of approximately 2–3·10^{-10} m (2–3 Å) (45, 46). The interaction between molecules, such as formation of DR complexes in the gas phase, can be described by means of total quantum chemical energies using the supermolecular approach as a difference between the total energies of the DR complex and the associating molecules:

$$\Delta E_{com}^{gas}=E_{DR}-E_D-E_R \qquad [8]$$

where E_{DR} is the total energy of DR and E_D and E_R are the energies of free (unbound) drug and receptor, respectively (see Figure 1).

If the total energies are amended by zero-point vibrational energies, then the quantity ΔE_{com}^{gas} corresponds to internal energy change at 0 K in the gas phase. However, ligands bind or form complexes with receptors in solution provided that the associated Gibbs free energy change of the binding is negative (at laboratory temperature, T, and pressure, P). The total electronic and nuclear energies from SCF or DFT calculation (E_{tot}) can be converted into thermodynamic quantities by assuming the classical ideal gas behavior of molecules and by performing the rigid rotor and harmonic vibrational analysis (48, 49):

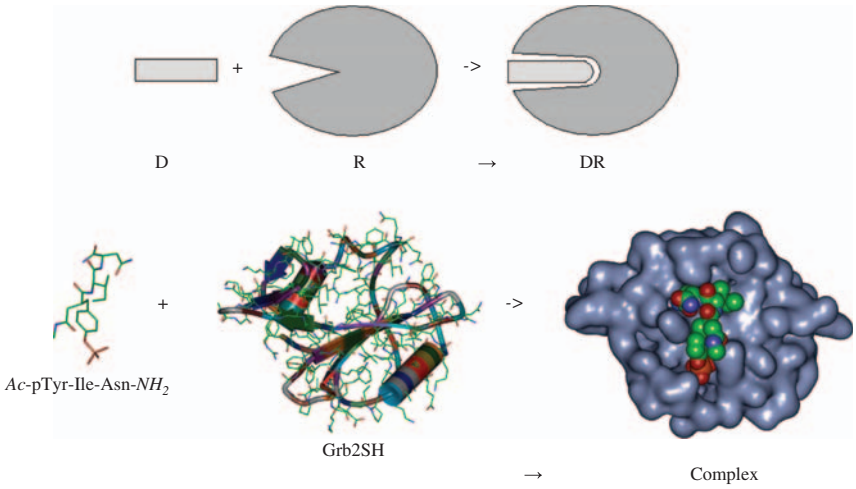

Figure 1 Scheme of induced fit mechanism of drug-receptor binding (above). Flexible tripeptide mimic *Ac-p*Tyr-Ile-Asn-NH_2 ligand binding to the sarcoma oncoprotein homology domain (SH) of growth factor receptor-bound protein 2 (47) (below).

$$G=E_{tot}+E_{ZPE}+E_e^T+E_t^T+E_r^T+E_v^T+RT-T(S_e^T+S_t^T+S_r^T+S_v^T)$$

$$\Delta G_{com}^{gas}=G_{DR}-G_D-G_R \qquad [9]$$

where E_{ZPE} is zero-point vibrational energy and E_i^T and S_i^T stand for the thermal correction of internal energy and entropy dependent on electronic states, translational, rotational and vibrational motions of the molecule, respectively (49). To derive the Gibbs free energy of the DR formation in solution $\left(\Delta G_{com}^{aq}\right)$, we can take advantage of a thermodynamic cycle (50), see Figure 2, and express the quantity as:

$$\Delta G_{com}^{aq}=\Delta G_{com}^{gas}+G_{sol}(DR)-G_{sol}(D)-G_{sol}(R) \qquad [10]$$

where ΔG_{com}^{aq} is the Gibbs free energy of complexation in aqueous solution, ΔG_{com}^{gas} is defined in Eq. [9] and $G_{sol}(X)$ is the solvation Gibbs free energy of the species X (Gibbs free energy of transfer from gas phase to solvent, Eq. [7]). To obtain the ΔG_{com}^{aq} we can model the process of drug-receptor association in the gas phase and include the Gibbs free energies of solvation of the DR, D and R species.

Similar equations can be derived for enthalpy $\left(\Delta H_{com}^{aq}\right)$ and entropy $\left(\Delta S_{com}^{aq}\right)$ of the DR formation. Studies on ligand-receptor binding in the gas phase suggest that $\left(\Delta H_{com}^{gas}\right)$ and $\left(\Delta S_{com}^{gas}\right)$ are always negative, i.e., the binding is driven by the exothermic D-R interaction. In solution, ΔH_{com}^{aq} and ΔS_{com}^{aq} can assume both negative and positive values and ligand-receptor binding can be driven either by the enthalpic or the entropic effect or both (51).

We should keep in mind that during the DR complex formation from solvated D and R species the thermodynamics of the process can also be dominated by changes in the solvent-solvent interactions, as it is known from the hydrophobic effect (association of nonpolar molecules in water) (52). In addition, we should be aware of the fact that the use of gas-phase entropies often leads to a significant overestimation of the entropy term for processes in solution (mainly due to the harmonic approximation, which underestimates the contribution of the low-frequency modes that are more abundant in larger solutes, such as DRs) (53, 54).

The ΔG_{com}^{aq} is a quantity computed for the optimized molecular geometry of a low energy conformation (ideally global minima on the conformational energy hypersurface) of the interacting D and R molecules and the resulting DR. To compare the theoretical quantity ΔG_{com}^{aq} with the observed dissociation constant of the complex: $\ln K_d=\Delta G_{bin}/RT$, which is measured on a macroscopic scale and reflects an ensemble average of the binding affinity (ΔG_{bin}) over a set of low energy conformations accessed in a dynamic equilibrium by the reactants and the complex at ambient temperature, we have to replace the single Gibbs free energy of complexation with an ensemble average: $\Delta G_{bin}=<\Delta G_{com}^{aq}>$. Thus, to calculate the ΔG_{bin}, we have to sample the conformational space of the reactants and products and replace the terms in Eq. [10] with ensemble averages over accessible low-energy conformational states.

Since larger ligands, and especially protein receptors, can acquire a vast number of conformations (configurations) with closely separated minima, it is necessary to use stochastic sampling as well as faster methods of calculation of molecular

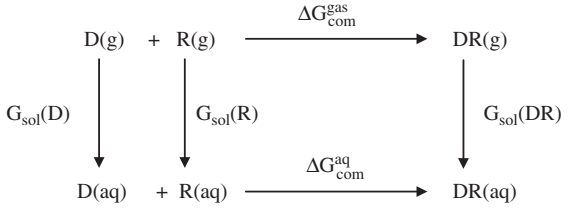

Figure 2 Thermodynamic cycle used to calculate the Gibbs free energies of drug-receptor association in solution (50).

internal energy and thermodynamic quantities, namely the so-called molecular simulation methods (55, 56).

Perturbation theory of intermolecular interactions

In biological and pharmacological applications, the SCF computation of E_{DR} and G_{DR} as well as direct estimate of the binding energy or Gibbs free energy for larger macromolecular receptors may become computationally expensive or even impossible. An estimate of the binding energy (ΔE_{com}^{gas}) of rigid interacting particles can, however, be obtained from the Rayleigh-Schrödinger perturbation theory of intermolecular interactions (45, 57–60). In this approach, for two interacting D and R particles, which obey the relations $\hat{H}^D\Psi^D=E^D\Psi^D$ and $\hat{H}^R\Psi^R=E^R\Psi^R$, the interaction energy between D and R can be determined by solving the Schrödinger equation with a total Hamiltonian composed of an unperturbed ($\hat{H}^0$) and interaction component ($\hat{U}$, the perturbation), given by:

$$\hat{H}=\hat{H}^D+\hat{H}^R+\hat{U}=\hat{H}^0+\hat{U}$$
$$=\hat{H}^0+\sum_i^D\sum_k^R\frac{e^2}{r_{ik}}-\sum_A^D\sum_k^R\frac{Z_Ae^2}{r_{Ak}}-\sum_i^D\sum_C^R\frac{Z_Ce^2}{r_{iC}}$$
$$+\sum_A^D\sum_C^R\frac{Z_AZ_Ce^2}{r_{AC}} \qquad [11]$$

where the summation indices i, k and A, C extend over the electrons and nuclei of the individual systems D and R. According to the polarization approximation of Hirschfelder (58, 59), the interaction energy $\left(\varepsilon_{DR}=\sum_{n=1}^{\infty}E_{pol}^{(n)}\right)$ and wave function $\left(\Phi_{DR}=\sum_{n=0}^{\infty}\Psi_{pol}^{(n)}\right)$, antisymmetrical with respect to electron exchange within the individual subsystems) are written as the sum of energies and wave functions of the n-th order of perturbation theory, yielding the following recurrent expressions:

$$E_{pol}^{(n)}=<\Psi^0|\hat{U}|\Psi_{pol}^{(n-1)}> \qquad \Psi_{pol}^{(n)}=-S_0\hat{U}\Psi_{pol}^{(n-1)}+\sum_{j=1}^{n-1}E_{pol}^{(j)}S_0\Psi_{pol}^{(n-1)}$$
$$\Psi_{pol}^{(n)}=\Psi^0=\Psi_0^D\Psi_0^R \qquad S_0=\sum_{K\neq0}\frac{|\Psi^K><\Psi^K|}{E_K-E_0} \qquad [12]$$

where E_K and Ψ^K are the eigenvalues and eigen functions of the Hamiltonian ($\hat{H}^0$), respectively.

When the polarization expansion [12] is combined with the electron exchange expansion terms (61, 62) derived from the perturbation theory that considers the wave function antisymmetric with respect to the exchange of all electrons, the interaction energy expansion converges for smaller systems in the region of van der Waals distances between D and R after the second-order terms (61–63). Based on the functional forms of the perturbation terms, approximate expressions have been proposed for the individual components contributing to the perturbation interaction energy, which include the Coulombic (E^C), induction (E^I), dispersion (E^D) and exchange-repulsion (E^{ER}) contributions composed of additive pair-wise atomic or bond contributions:

$$E^{INT}=E^C+E^I+E^D+E^{ER}=$$
$$\frac{1}{2}\sum_s^D\sum_t^R\frac{Q_sQ_t}{4\pi\varepsilon_0r_{st}}-\frac{1}{2}\left\{\sum_q^R[\alpha_q^t(\boldsymbol{\beta}_q\boldsymbol{\beta}_q)+\delta_q(\boldsymbol{\beta}_q\boldsymbol{\alpha}_q^l)^2]+\right.$$
$$\left.\sum_p^D[\alpha_p^t(\boldsymbol{\beta}_p\boldsymbol{\beta}_p)+\delta_p(\boldsymbol{\beta}_p\boldsymbol{\alpha}_p^l)^2]\right\}-$$
$$\frac{1}{4}\frac{\bar{E}_D\bar{E}_R}{\bar{E}_D+\bar{E}_R}\sum_p^D\sum_q^R\frac{1}{r_{pq}^6}\left\{6\alpha_q^t\alpha_p^t+\alpha_q^t\delta_q[3(\boldsymbol{\alpha}_p^l\mathbf{r}_{pq})^2+1]+\right.$$
$$\left.\alpha_p^t\delta_q[3(\boldsymbol{\alpha}_p^l\mathbf{r}_{pq})^2+1]+\delta_p\delta_q[3(\boldsymbol{\alpha}_q^l\mathbf{r}_{pq})(\boldsymbol{\alpha}_p^l\mathbf{r}_{pq})-(\boldsymbol{\alpha}_q^l\boldsymbol{\alpha}_p^l)]^2\right\}+ \qquad [13]$$
$$\sum_s^D\sum_t^Rb_{st}\exp\left[-c_{st}\left(\frac{r_{st}}{R_s+R_t}\right)\right]-\sum_s^D\sum_t^Ra_{st}\left[\frac{R_s+R_t}{r_{st}^6}\right]^6$$

where:

- summation indices p, q run over bonds and s, t over the atoms of systems D and R;
- r_{st} is the interatomic distance;
- Q_i are atomic charges;
- r_{pq} is distance between the centers of bonds p and q and $\mathbf{r}_{pq}$ is the corresponding unit vector;
- α_i^t and α_i^l are the transversal and longitudinal components of polarizability of bond i, $\delta_i=\alpha_i^l-\alpha_i^t$;
- $\bar{E}_i$ is the average excitation energy of system i;
- $\boldsymbol{\alpha}_i^l$ is a unit vector in the direction of bond i, $\boldsymbol{\beta}_q=\sum_p^D\frac{Q_p}{r_{pq}^3}\mathbf{r}_{pq}$;
- R_i is van der Waals radius of atom i; and
- a_{st}, b_{st}, and c_{st} are constants.

The atomic charges are usually determined by the ab initio method for the subsystems or their building blocks (e.g., amino acids). Atomic van der Waals radii and bond polarizabilities of distinct bonds are given in the literature (64). Ionization potentials may come from the experiment or can be derived by quantum chemical calculations.

This "monopole-bond polarizability" method is numerically simple, also permitting calculations of interaction energy for large macromolecular systems (45). When the overlap of the charge distributions of the subsystems D and R is negligible, then the long-range electrostatic interaction term E^C can be more precisely described by the multipole expansion, which includes also higher moments (dipole, quadrupole, etc.) (45).

Force fields

In molecular modeling of systems of pharmacological interest, we frequently encounter situations when realistic models of biological/biochemical processes are too large to be treated by quantum chemical methods. Force field (FF) methods (also known as molecular mechanics, MM) ignore the motions of electrons and calculate the potential energy of a system analytically using an empirical potential energy expression as a function of nuclear positions (11). A relatively simple chemical potential energy function (defined for internal molecular coordinates) is composed of bonding terms that reflect the energies of basic molecular motions (bond stretching $V_b(1)$, bond angle bending $V_a(\theta)$, torsion angle rotation $V_t(\omega)$, etc.)

and nonbonding interatomic interactions [Coulombic $V_{el}(r_{ij})$, van der Waals $V_{LJ}(r_{ij})$, hydrogen bonding $V_{hb}(d_{ij})$] between atoms that are not directly bonded:

$$U(x_1,\ldots,x_{3N})=$$
$$\frac{1}{2}\sum_{bon} k_{li}(l_i-l_{0i})^2+\frac{1}{2}\sum_{ang} k_{\theta i}(\theta_i-\theta_{0i})^2+$$
$$\frac{1}{2}\sum_{tor} V_{ni}[1+\cos(n\omega_i-\gamma_i)]+$$
$$\sum_i\sum_{<j}\left\{\left[\frac{q_iq_j}{4\pi\varepsilon_0 r_{ij}}\right]+\left[\frac{A_{ij}}{r_{ij}^{12}}-\frac{B_{ij}}{r_{ij}^{6}}\right]+\left[\frac{C_{ij}}{d_{ij}^{12}}-\frac{D_{ij}}{d_{ij}^{10}}\right]\right\}= \quad [14]$$
$$V_b(1)+V_a(\theta)+V_t(\omega)+V_{el}(r_{ij})+V_{LJ}(r_{ij})+V_{hb}(d_{ij})$$

Equation [14] estimates the potential energy penalty associated with the deviation of bond lengths, bond angles and torsion angles from their equilibrium values as well as the interactions between nonbonded parts of the system. The parameters of individual FF functional forms (constants, such as k_{li}, $k_{\theta i}$, V_{ni}, l_{0i}, θ_{0i}, γ_i, A_{ij}, B_{ij}, C_{ij} and D_{ij} pertinent to certain atom types), are obtained by parameterization against experimental data, as molecular geometries, heats of formation, heats of vaporization, vibrational frequencies and data predicted from high-level ab initio calculations for a class of molecules (11, 65).

Functional forms of the individual potential energy components are chosen so as to allow easy analytical formulation of forces acting on the atoms: $f_{x_i}=-\frac{\partial U(x_1,\ldots,x_{3N})}{\partial x_i}$, which are used in geometry optimization and molecular dynamics simulations.

The transferability of simple FF parameters between different sets of molecules is limited and FF can be used for modeling of related molecules. Classical FFs, which use isotropic pair-wise potentials and fixed atomic charges, fail in situations where the change of an atom type is required (e.g., chemical reactions), however, they provide useful insights into and interpretation of biomolecular structure and function.

A relatively large number of specialized and general FFs have been developed for different purposes: modeling and simulations of proteins, nucleic acids, saccharides, lipids, zeolites, small organic molecules, inorganic molecules, and water, see Table 2 (66). Modern polarizable FFs use induced dipoles, distributed multipoles, density fitting, bond-polarization or explicit polarization to represent the dynamic character of molecular charge density. Reactive FFs, such as ReaxFF based on continually updated bond orders instead of explicit atom connectivity definition (67), show the future directions in the effort to overcome the drawbacks of classical FFs.

Molecular simulations

The two most common simulation techniques used in molecular modeling are the molecular dynamics (MD) and Monte Carlo (MC) methods. The former method tracks the time-evolution of the system, samples the phase space along a trajectory (contour of constant energy in NVE ensemble) and permits the calculation of time-averaged physicochemical properties ($\bar{A}$) over the MD simulation time.[6] The later method randomly samples the configuration space and provides ensemble-averaged properties (<A>) over the number of collected configurations ($\bar{A}$ is equivalent to <A>, ergodic hypothesis) (11).

In the MD simulation, successive atomic configurations are generated by numerically integrating Newton's equations of motion with a very short time step (δt=1fs) in a constantly changing potential energy (force field):

$$a_{x_i}=\frac{d^2x_i}{dt^2}=\frac{f_{x_i}}{m_i}=-\frac{\partial U(x_1,\ldots,x_{3N})}{m_i\partial x_i}$$
$$x_i(t+\delta t)=2x_i(t)-x_i(t-\delta t)+\delta t^2 a_{x_i}(t)$$
$$v_{xi}(t)=\frac{[x_i(t+\delta t)-x_i(t-\delta t)]}{2\delta t} \quad [15]$$

where the forces $\mathbf{f}_i=(f_{x_{i1}},f_{x_{i2}},f_{x_{i3}})$ acting on the atoms are obtained as the gradient of the potential $U(x_1,\ldots,x_{3N})$, Eq. [14]. The atomic position vectors $\mathbf{r}_i=(r_{x_{i1}},r_{x_{i2}},r_{x_{i3}})$ and velocities $\mathbf{v}_i=(v_{x_{i1}},v_{x_{i2}},v_{x_{i3}})$ can be obtained, for example, from the Verlet algorithm, Eq. [15] (68) and are stored as the simulation trajectory. The Verlet integration algorithm is relatively simple, fast and stable for short integration time-steps (1–10 fs) (69). The simulation starts from a selected system configuration ($\{\mathbf{r}_{i0}\}$) and the initial velocities $\{\mathbf{v}_{i0}\}$ are assigned from Maxwell-Boltzmann distribution at a given temperature.

The Metropolis MC method (70) generates system configurations randomly by varying the positions and orientation of one or more atoms in the present configuration and uses a Boltzmann factor (f_{Bol}) criterion dependent on potential energy computed from the FF to decide whether or not to accept a new configuration:

$$f_{Bol}=\exp\left[\frac{U_{new}(x_1,\ldots,X_{3N})-U_{old}(x_1,\ldots,X_{3N})}{RT}\right]\leq f_{ran} \quad [16]$$
$$f_{ran}\in<0,1>$$

If the U_{new} is lower than U_{old} (present configuration) then the new configuration is accepted. If U_{new} is higher than U_{old} and f_{Bol} is lower than a random number f_{ran}, then the new configuration is still accepted and becomes the present one, otherwise it is rejected. This criterion has the effect of permitting moves to higher energy states, however, acceptance of smaller uphill moves has a higher probability then the larger jumps on the energy scale (importance sampling) (71).

The inclusion of velocities and kinetic energy into the MD simulations allows the system to overcome energy

[6] A thermostat or barostat can be applied to allow constant temperature or pressure MD simulations.

[7] In classical mechanics, Hamiltonian is a function of total energy: $H(p,q,t)=\sum_i^{3N}\frac{p_i^2(t)}{2m_i}+V(q_1(t),\ldots,q_{3N}(t))$, where $q_i(t)$ are time-dependent coordinates and $p_i(t)$ denote the momenta of atoms.

Table 2 List of acronyms of selected popular force fields.

Classical	Second generation	Polarizable	Reactive	Coarse grain
AMBER	CFF	AMBER/pol	EVB	VAMM
CHARMM	MMFF	AMOEBA	ReaxFF	
CVFF	MM2,MM3,MM4	CHARMM/pol	RWFF	
Dreiding	QVBMM	CFF/ind		
ECEPP/2		COSMOS-NMR		
ENCAD		DRF90		
GROMACS		ENZYMIX		
GROMOS		GEM		
OPLS		NEMO		
QCFF/PI		ORIENT		
TRIPOS		PIPF		
UFF		PPF		
		SIBFA		
		SP-basis		
		X-pol		

barriers of the height of k_BT per degree of freedom. Despite this, at the laboratory temperature the system will predominantly sample the low-energy regions of the phase space and therefore the free energy of the system (ΔG at constant NPT) calculated using conventional MD simulation will not be very accurate. However, when studying system B with the help of a similar reference system A (such as a lead compound and its analog) described by Hamiltonians H_A and H_B[7], the Gibbs free energy difference between B and A can be expressed as: $\Delta G_{BA}=G_B-G_A=RT\ln\langle e^{\left(-\frac{\Delta H_{BA}}{RT}\right)}\rangle_B$ as an ensemble average corresponding to the final state ($\Delta H_{BA}=H_B-H_A$) (72). The relation between the final and the initial state is usefully described by a coupling parameter λ as: $H(\lambda)=\lambda H_B+(1-\lambda)H_A$, where λ changes from 0 ($H=H_A$) to 1 ($H=H_B$) and

$$\Delta G_{BA}=G_B-G_A=\sum_{\lambda=0}^{\lambda=1}\left[-RT\ln\langle e^{\left(-\frac{\Delta H_\lambda}{RT}\right)}\rangle_\lambda\right],$$

where $\Delta H_\lambda=H_{\lambda+d\lambda}-H_\lambda$.This is the basic equation of the free energy perturbation (FEP) method. The Gibbs free energy difference ΔG_{BA} is then accumulated as a string of increments $\Delta G(\lambda_i\rightarrow\lambda_i+d\lambda)$ obtained from a series of MD simulations performed for the system with parameter λ increasing gradually from 0 to 1 with a small step of $d\lambda$ (see Figure 3). Thus, larger free energy changes must be calculated using N independent MD simulations with different λ values while the free energy difference should be in the order of k_BT for each run (73, 74).

An alternative way to calculate the free energy difference is to employ the thermodynamic integration (TI), which uses the following formula for the Gibbs free energy difference ΔG_{BA}:

$$\Delta G_{BA}=\int_{\lambda=0}^{\lambda=1}\left\langle\frac{\partial H_\lambda}{\partial\lambda}\right\rangle_\lambda d\lambda \qquad [17]$$

This integral is determined in practice by performing a series of MD simulations for discrete values of parameter λ, ranging from 0 to 1, and computing the ensemble averages $\langle\partial H/\partial\lambda\rangle_\lambda$ for each value of λ, see Figure 3 (75). Various other statistical mechanical methods of computing the free energy difference from MD or MC simulations exist, such as the slow growth method, umbrella sampling and others (76).

Perhaps the most relevant application of the free energy techniques is the prediction of the binding affinity of ligands

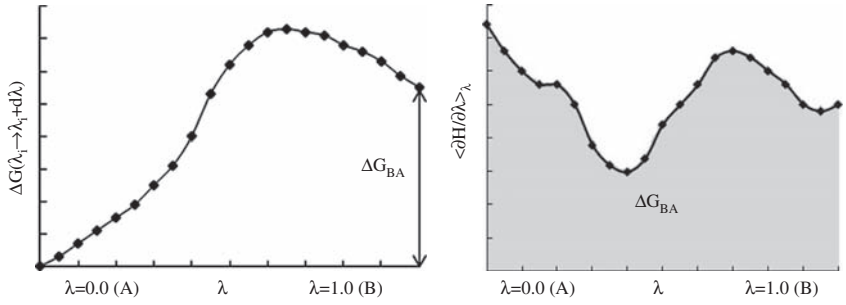

Figure 3 Calculation of the difference in Gibbs free energy between molecules A and B using free energy perturbation method (left) and thermodynamic integration (right) (11).

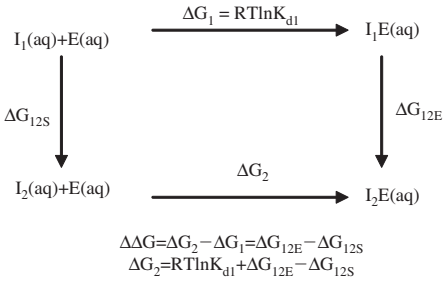

Figure 4 Thermodynamic cycle for binding of reversible inhibitors I_1 and I_2 to enzyme E in solution. K_{d1} is the experimental dissociation constant of the I_1E complex.

to their receptors. Provided that dissociation constant K_d of a known inhibitor I_1 has been experimentally determined, we can predict the binding constant of an analog I_2 from a thermodynamic cycle (see Figure 4) by performing two separate FEP calculations. In the first computer experiment we mutate inhibitor I_1 into I_2 in solution with the help of the coupling parameter λ. In the second one, we model the mutation at the binding site of the solvated enzyme. These two transformations cannot be performed in laboratory, but can be carried out computationally much more easily than by running the simulation of the actual binding process. This would require a simulation of the approach of the interacting particles from an initially large separation, simulation of conformational changes of the enzyme connected with the inhibitor binding, and reorganization of the solvent and the inhibitor. It would be difficult to ensure adequate sampling of the phase space for such a complex process (11). The simulated nonphysical transformation, however, typically corresponds to an addition or a replacement of a function group on the reference molecule I_1.

Since Gibbs free energy is a state function, we can predict the binding affinity of the I_2 from the closed thermodynamic cycle, see Figure 4 (77, 78). The free energy can be decomposed into additive contributions from different groups of atoms and types of interactions, which sets a firm basis for rational drug design (79). The FEP methods are computationally intensive and are inappropriate for the estimation of binding affinity differences between structurally dissimilar ligands.

QM/MM methods

In complex biological processes – such as the binding of a substrate to the active site of an enzyme – that are connected with the breaking or formation of chemical bonds, charge transfer, change of oxidation state and other quantum effects, the models are too large and computationally expensive for rigorous ab initio calculations. These processes can, however, be described by hybrid quantum mechanical/molecular mechanical (QM/MM) methods (80–82). In this approach, the core of the system (e.g., catalytic site of an enzyme including the substrate, the quantum motif) is treated quantum mechanically with the rest of the system (more distant parts of the protein structure and the solvent) described by FF methods, see Figure 5 .

The whole system can be embedded in solvent (surroundings), treated either explicitly or via continuum, Poisson-Boltzmann or Langevin models of solvation (34, 40, 42). The division of the system into individual parts is somewhat arbitrary and follows the goal of the highest possible precision of results at the lowest computational expense. Systems described by hybrid QM/MM potentials can use effective Hamiltonians ($\hat{H}_{eff}$):

$$\hat{H}_{eff}=\hat{H}_{QM}+\hat{H}_{MM}+\hat{H}_{QM/MM}+\hat{H}_{Sur}$$

$$\hat{H}_{QM/MM}=-\sum_i\sum_M\frac{eq_M}{r_{iM}}+\sum_\alpha\sum_M\frac{Z_\alpha eq_M}{r_{\alpha M}}+\sum_\alpha\sum_M\left[\frac{A_{\alpha M}}{R_{\alpha M}^{12}}-\frac{B_{\alpha M}}{R_{\alpha M}^{6}}\right] \quad [18]$$

where:

- $\hat{H}_{QM}$ is the standard electronic Hamiltonian of the QM motif (Eq. [3]);
- $\hat{H}_{MM}$ represents the interactions between atoms of the MM part only and is equal to the MM potential energy (Eq. [14]);
- $\hat{H}_{Sur}$ denotes the interaction with the surroundings (solvent) and can be replaced, e.g., by the reaction field Hamiltonian $\hat{H}_{RF}$ (Eq. [6]).

The effect of the surroundings on the MM motif is computed classically and is added to the E_{MM} – the energy of the MM part. Finally, $\hat{H}_{QM/MM}$ stands for the interaction between

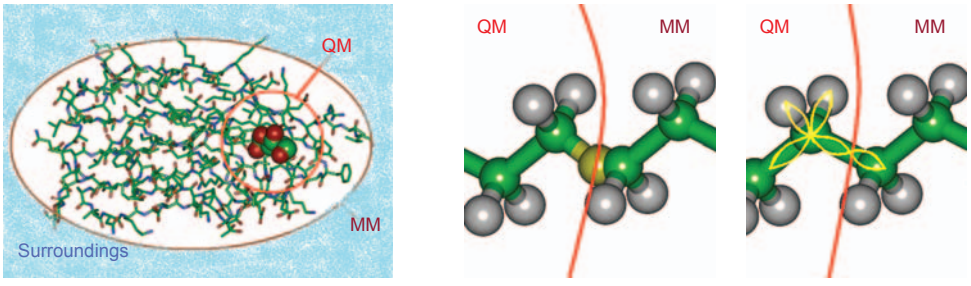

Figure 5 Division of the system studied into quantum mechanical (QM), molecular mechanical (MM) and boundary regions (left). Connection between QM and MM regions in a macromolecule is made by a dummy hydrogen atom – yellow (middle) – or by a single hybrid sp^3 atomic orbital at bonded MM carbon at the boundaries between QM and MM regions (right).

the MM and QM motifs. In this case, atoms of the MM part act upon the QM motif via electrostatic and dispersion-repulsion (Lennard-Jones) interactions (i and α represent electrons and nuclei of the QM and M refers the atoms of the MM motif, respectively). Several methods of QM and MM motifs coupling have been proposed. For example, we may consider atomic dipoles ($\boldsymbol{\mu}_M$) on the MM atoms induced by the electrostatic field ($\mathbf{E}_M$) deriving from the QM motif: $\boldsymbol{\mu}_M=\alpha_M\mathbf{E}_M$ (α_M is atomic isotropic polarizability). However, since the energies of the QM and MM motif are inter-dependent due to mutual polarization the computational times in such settings can increase significantly.

In relatively simple systems describing reactions between small molecules, the critical QM motif is typically composed of the reacting particles while the solvent is attributed to the MM motif. However, in reactions involving enzymes, the boundaries between the motifs cut through the covalent bonds of the macromolecule, see Figure 5. To compensate for the incomplete connecting bonds, Singh and Kollman introduced dummy hydrogen atoms to fill the valency of the boundary QM atoms (81). Warshel and Levitt (80) used another approach and placed a hybrid sp^3 orbital filled with one electron on the directly bonded MM atom to simulate the connecting σ-bond (see Figure 5).

Morokuma and co-workers developed another hybrid method, ONIOM[8], that allows the application of different levels of theory to defined layers of the system being modeled (83, 84). This approach, implemented in Gaussian 09 (85), can serve for the geometry optimization and property description of larger systems of chemical and biological interest (86, 87).

MM-PBSA/GBSA

The molecular mechanics-Poisson Boltzmann surface area/generalized Born surface area (MM-PBSA/GBSA) approach represents a computationally efficient FF-based method to evaluate free energies of binding. It combines atomic detail molecular dynamics simulations with implicit solvation models (88, 89). The approach uses a thermodynamic cycle (see Figure 2) to derive the Gibbs free energy of ligand-receptor binding in solution, ΔG^{aq}_{com}, Eqs. [9] and [10]. The molecular structures are obtained and averaged over a set of representative MD or MC snapshots. The Gibbs free energies of the interacting particles in the gas phase: $G^{gas}=E_{MM}-TS_{vib}$ amend the MM total energies with the entropic contribution deriving from the normal mode analysis. Solvation Gibbs free energies: $G_{sol}=G_{els}+G_{hfob}$ are composed of an electrostatic component, calculated by solving the linearized Poisson Boltzmann equation (40) or by the generalized Born expression (41), and an estimate of the nonpolar free energy of solvation approximated by a simple surface area term (G_{hfob}) (90).

The MM-PBSA method calculates the absolute Gibbs free energy of ligand–receptor association directly as the difference between the reactants and products, which is connected with much larger errors than the FEP or TI calculations. Nevertheless, despite the larger uncertainties, this relatively fast method which is applicable to small-to-medium size sets of designed drug candidates can often calculate binding affinities of ligand-receptor, protein-protein and DNA-protein association in respectable agreement with experiments (91, 92).

Linear interaction energy

The linear interaction energy (LIE) method is suitable for the calculation of binding free energies of various ligands (93, 94). LIE averages interaction energies obtained from MD or MC simulations (conformational sampling) of free particles and the bound state (DR). The idea behind the LIE method – the linear response approximation – assumes that it is sufficient to evaluate only convergent averages of the interaction energies between the ligand and its surroundings to obtain an estimate of the binding affinity to the receptor:

$$\Delta G_{bin}=\alpha[<E_{vdW}>_b-<E_{vdW}>_f]+\beta[<E_{els}>_b-<E_{els}>_f]+\gamma \quad [19]$$

Here $<E>_x$ denotes ensemble averages of the van der Waals (vdW) and electrostatic (els) interaction energy components over a collected set of configurations, where the subscript b (bound) refers to the DR where the ligand interacts with the receptor, solvent, co-factors, ions, etc., while the subscript f (free) means that it interacts with the solvent and salt ions only.

Two simulations have to be carried out: one with the free ligand in solution and one with the ligand bound to the solvated receptor. In Eq. [19], the α, β and γ are empirical coefficients obtained by fitting experimentally determined values of ΔG_{bin} to the calculated values of E_{vdW} and E_{els} for a training set of known ligands. Åqvist and co-workers claim that the values of these parameters are neither system-dependent nor FF dependent for ligand-protein systems (95, 96). Other authors have concluded that the LIE method has failed to reproduce the experimental binding constants (97). Nevertheless, the combination of docking and LIE affinity predictions has been shown to be useful in the design and optimization of drugs (98, 99).

The linear response approximation was amended by the preorganized electrostatics model, which suggests that proteins, in contrast to polar solvents, are electrostatically preorganized to accommodate their ligands (dipoles associated with polar function groups and ionized residues of the receptor binding site are oriented favorably during the protein folding). By analyzing the antigen-antibody interactions Lee et al. (100) concluded from component analysis of the different energy contributions to the ligand binding affinity that electrostatic effects provide the largest contribution to the differential binding energy, while the hydrophobic and steric contributions are much smaller.

MM-PCM

The molecular mechanics-polarizable continuum model of solvation (MM-PCM) is another method of calculating the relative Gibbs free energy of receptor binding, which

[8]Our own N-layered Integrated molecular Orbital and molecular Mechanics (83, 84).

is applicable to similar analogs (101). In this approach, the crystal structure of a ligand-receptor complex is modified in situ to transform the native ligand into an analog. Then an exhaustive conformational search of the replacing functional groups is carried out to select the best rotamers. Low energy states of flexible ligand and receptor (flexibility of receptor is typically restricted to the binding site) are explored by simulated annealing. The relative Gibbs free energy of the ligand-receptor binding in solution, $\Delta\Delta G^{aq}_{com}$, with respect to a reference ligand (L_r), is obtained from Gibbs free energies of the solvated particles, using the supermolecular method, Eqs. [8–10], as:

$$\Delta G^{aq}_{com}(L) - \Delta G^{aq}_{com}(L_r) = \Delta\Delta G^{aq}_{com} = \Delta\Delta H_{MM} + \Delta\Delta G_{sol} - T\Delta\Delta S_{vib}$$
$$\Delta\Delta H_{MM} = [(E_{MM}(LR) - E_{MM}(R) - E_{MM}(L) - RT] - \Delta H_{MM}(L_r)$$
$$\Delta\Delta G_{sol} = [G_{elst}(L) + G_{disp,rep}(L) + G_{cav}(L)] - \Delta G_{sol}(L_r) \quad [20]$$
$$T\Delta\Delta S_{vib} = [TS_{vib}(L)_{Rec} - TS_{vib}(L)] - T\Delta S_{vib}(L_r)$$

The enthalpic contribution is equal to the difference in the MM total energies of the associating particles. The solvent effect is described by the PCM of solvation (37, 38, 102–106) and includes electrostatic, dispersion–repulsion and cavitation contributions, see Eq. [7] (34, 102). The entropic contribution to the binding affinity is computed by normal mode analysis of the involved species, or eventually for very large protein molecules the frozen receptor approximation of Fischer et al. (107) can be employed.

The relatively computationally inexpensive MM-PCM method is applicable to larger series of analogs and has been used in the structure-based design of antiviral and antibacterial compounds (108–111). The precision of the predicted binding affinities can be improved by a calibration study on a test set of similar ligands, for which experimentally determined K_ds are available.

Docking and scoring functions

Molecular docking and scoring play significant roles in the prediction of ligand-receptor binding and virtual screening of combinatorial libraries (112, 113). Numerous docking algorithms that generate ligand poses (relative position, orientation and conformation) within the receptor's binding site and explore the conformational space of the ligand and receptor have been proposed (114, 115). The flexible ligand docking methods include matching algorithm, incremental construction, stochastic methods (MC, genetic algorithm, simulated annealing, and tabu search), multistep procedures and consensus docking.

The flexibility of the receptor's binding site (an essential feature of the induced fit mechanism) is also taken into account. This is done either by docking the ligand into multiple receptor configurations obtained, for example, from MD simulations or by allowing for the flexibility of a limited number of the side chains of selected active site residues in a single receptor configuration. More than 60 docking programs exist and about a dozen of them (AutoDock, DOCK, FlexX, FRED, FTDock, Glide, GOLD, ICM, LigandFit, QXP/Flo+, SLIDE, Surflex and ZDOCK) are used more widely (115). Each docking program relies on a scoring function (SF – an empirical or knowledge-based potential energy function) to evaluate the generated ligand poses. The suitable SF should assign a high score to the correct pose (the native pose observed in crystal structure of the ligand-receptor complex), which is critical for accurate prediction of the binding mode for analog docking. In addition, the docked poses of highly active compounds should be attributed better scores than those of nonbinders or poor binders, which is important for the identification of potential hits during virtual library screening. SFs take the functional form similar to the perturbation treatment of the intermolecular interaction energy (Eq. [13]), common to the nonbonding part of many FFs. SFs are usually calibrated on a set of ligand–receptor crystal structures to reproduce the experimental binding affinities. More than 30 different SFs have been published and about 12 of them (AutoDock, ChemScore, DrugScore, FlexX, GlideScore, GoldScore, HINT, ICM, LigScore, LUDI, PLP, PMF, and Validate) are more popular (115).

While the speed of the molecular docking and scoring run is essential for an effective virtual high-throughput screening of large libraries, the accuracy is critical for the lead optimization. Comparative studies (116–118), the only available tools to evaluate relative performance of the docking programs and the SFs, suggest that none of the algorithms or SFs clearly outperformed the others. The comparisons did, however, show that significant improvements must still be achieved in order to develop universal, fast and highly accurate docking/scoring methods.

Conclusions

Constant improvements in the methods and modeling algorithms, as well as the reduction in the cost of high-performance computing, are ensuring that systems of increasing size and therefore interest to structural biology and pharmacology will become amenable to molecular modeling. These will thus allow us to advance towards the ultimate goal of theoretical approaches: achieving full partnership with the experiment as both an explanatory and predictive methodology (18). We can expect a number of new applications of computational predictions of drug-receptor interactions to be carried out in the years to come, especially in the fields of virtual screening, lead optimization and structure-based drug design.

Acknowledgements

This work was supported by grants from The Slovak Research and Development Agency under the contract VVCE-0001-07 and by VEGA grant 2/0153/11.

Conflict of interest statement

Author's conflict of interest disclosure: The author stated that there are no conflicts of interest regarding the publication of this article. Research support played no role in the study design; in the collection,

analysis, and interpretation of data; in the writing of the report; or in the decision to submit the report for publication.

Research funding: None declared.
Employment or leadership: None declared.
Honorarium: None declared.

References

1. Rose RS, Golan DE. Pharmacodynamics. In: Golan DE, Tashijian AH Jr, Armstrong EJ, Armstrong AW, editors. Principles of pharmacology: the pathophysiologic basis of drug therapy, 2nd ed. Baltimore, MD: Wolters Kluwer, Lippincott, Williams & Wilkins, 2008:19–30.
2. Riley KE, Hobza P. Noncovalent interactions in biochemistry. WIREs Comput Mol Sci 2011;1:3–17.
3. Davis AM, Teague SJ, Kleywegt GJ. Application and limitations of X-ray crystallographic data in structure-based ligand and drug design. Angew Chem Int Ed Engl 2003;42:2718–36.
4. Wider G. Structure determination of biological macromolecules in solution using NMR spectroscopy. Biotechniques 2000;29:1278–94.
5. Tramontano A, Morea V. Assessment of homology-based predictions in CASP5. Proteins 2003;53:S6:352–68.
6. Diller DJ, Verlinde CL. A critical evaluation of several global optimization algorithms for the purpose of molecular docking. J Comp Chem 1999;20:195–202.
7. Xu Y, Colletier JP, Jiang H, Silman I, Sussman JL, Weik M. Induced-fit or preexisting equilibrium dynamics? Lessons from protein crystallography and MD simulations on acetylcholinesterase and implications for structure-based drug design. Protein Sci 2008;17:601–5.
8. Koshland DE. Application of a theory of enzyme specificity to protein synthesis. Proc Natl Acad Sci USA 1958;44:98–104.
9. Monod J, Wyman J, Changeux JP. On the nature of allosteric transitions: a plausible model. J Mol Biol 1965;12:88–118.
10. Watson JD. Molecular biology of the gene. Benjamin, New York, NY, 1965.
11. Leach AR. Molecular modelling: principles and applications, 2nd ed. Prentice Hall, Englewood Cliffs, NJ, 2001.
12. Szabo A, Ostlund NS. Modern quantum chemistry. New York, NY, MacMillan: 1982.
13. Hartree DR. The wave mechanics of an atom with a non-coulomb central field. Part I. Theory and methods. Proc Cambridge Phil Soc 1928;24:89–110.
14. Fock V. Näherungsmethode zur Lösung des quantenmechanischen Mehrkörperproblems. Z Physik 1930;61:126–48.
15. Hall GG. The molecular orbital theory of chemical valency VIII. A method of calculating ionization potentials. Proc Roy Soc London A 1951;205:541–52.
16. Roothaan CC. New development in molecular orbital theory. Rev Mod Phys 1951;23:69–89.
17. Čársky P, Urban M. Ab Initio calculations: methods and applications in chemistry. Berlin, Springer-Verlag: 1980.
18. Friesner RA. Ab initio quantum chemistry: methodology and applications. Proc Natl Acad Sci USA 2005;102:6648–53.
19. Clark T. A handbook of computational chemistry. New York, NY, John Wiley & Sons: 1985.
20. Dewar MJ, Thiel W. Ground states of M\molecules. 38. The MNDO method. Approximations and parameters. J Am Chem Soc 1977;99:4899–907.
21. Stewart JJ. Special issue – MOPAC – a semiempirical molecular-orbital program. J Comput Aided Mol Des 1990;4:1–45.
22. Rocha GB, Freire RO, Simas AM, Stewart JJ. RM1: a reparameterization of AM1 for H, C, N, O, P, S, F, Cl, Br, and I. J Comput Chem 2006;27:1101–11.
23. Stewart JJ. Optimization of parameters for semiempirical methods V: modification of NDDO approximations and application to 70 elements. J Mol Modeling 2007;13:1173–213.
24. Levine IN. Quantum chemistry, 4th ed. Prentice-Hall, Englewood Cliffs, NJ, 1991.
25. Cramer CJ. Essentials of computational chemistry. Chichester, John Wiley & Sons: 2002.
26. Møller C, Plesset MS. Note on an approximation treatment for many-electron systems. Phys Rev 1934;46:618–22.
27. Riley KE, Hobza P. Noncovalent interaction in biochemistry. Comput Mol Sci 2011;1:3–17.
28. Parr GR, Yang W. Density-functional theory of atoms and molecules. Oxford University Press, Oxford, 1994.
29. Hohenberg P, Kohn W. Inhomogeneous electron gas. Phys Rev B 1964;136:864–71.
30. Becke AD. Density-functional exchange-energy approximation with correct asymptotic behavior. Phys Rev A 1988;38:3098–100.
31. Perdew JP, Wang Y. Accurate and simple analytic representation of the electron-gas correlation energy. Phys Rev B 1992;45:13244–9.
32. Lee C, Yang W, Parr RG. Development of the Colle-Salvetti correlation-energy formula into a functional of the electron density. Phys Rev B 1988;37:785–9.
33. Oliphant N, Bartlett RJ. A systematic comparison of molecular properties using Hartree-Fock, a hybrid Hartree-Fock density-functional-theory, and coupled-cluster methods. J Chem Phys 1994;100:6550–61.
34. Tomasi J, Persico M. Molecular interaction is solution. An overview of methods based on continuous distribution of the solvent. Chem Rev 1994;94:2027–94.
35. Warshel A. Calculations of chemical processes in solutions. J Phys Chem 1979;83:1640–52.
36. Jorgensen WL, Buckner JK. Use of statistical perturbation theory for computing solvent effects on molecular conformation. Butane in water. J Phys Chem 1987;91:6083–5.
37. Miertus S, Scrocco E, Tomasi J. Electrostatic interaction of a solute with a continuum. A direct utilization of ab initio molecular potentials for the prevision of solvent effects. Chem Phys 1981;55:117–29.
38. Miertus S, Tomasi J. Approximate evaluations of the electrostatic free energy and internal energy changes in solution processes. Chem Phys 1982;65:239–45.
39. Thole BT, van Duijnen PT. Reaction field effects on proton transfer in the active site of actinidin. Biophys Chem 1983;18: 53–9.
40. Gilson MK, Honig B. Calculation of the total electrostatic energy of a macromolecular system: solvation energies, binding energies, and conformational analysis. Proteins 1988;4:7–18.
41. Dixit SB, Jayaram B. Role of hydrogen bonds in protein-DNA recognition: a comparison of generalized born and finite difference Poisson-Boltzmann solvation treatments. J Biomol Struct Dyn 199;16:237–42.
42. Florian J, Warshel A. Langevin dipoles model for ab initio calculations of chemical processes in solution: parameterization and application to hydration free energies of neutral and ionic solutes, and conformational analysis in aqueous solution. J Phys Chem B 1997;10:5583–95.
43. Schlegel HB. Optimization of equilibrium geometries and transition structures, In: Lawley KP: editor. Ab Initio methods in quantum chemistry – I. New York, NY, John Wiley: 1987:249–86.

44. Wilson S. Chemistry by computer. New York, NY, Plenum Press: 1986.
45. Hobza P, Zahradnik R. Intermolecular complexes. Prague, Academia: 1988.
46. Levitt M, Sharon R. Accurate simulation of protein dynamics in solution. Proc Natl Acad Sci USA 1988;85:7557–61.
47. Delorbe JE, Clements JH, Teresk MG, Benfield AP, Plake HR, Millspaugh LE, et al. Thermodynamic and structural effects of conformational constraints in protein-ligand interactions. Entropic paradoxy associated with ligand preorganization. J Am Chem Soc 2009;131:16758–70.
48. Foresman JB, Frisch A. Exploring chemistry with electronic structure methods, 2nd ed. Pittsburgh, PA, Gaussian: 1996.
49. McQuarrie DA. Statistical thermodynamics. Mill Valley, CA, University Science Books: 1973.
50. Jorgensen WL, Buckner JK, Boudon S, Tirado-Reeves J. Efficient computation of absolute free energies of binding by computer simulations. Applications to the methane dimer in water. J Chem Phys 1988;89:3742–6.
51. Wittmann H-J, Seifert R, Strasser A. Contribution of binding enthalpy and entropy to affinity of antagonist and agonist binding at human and guinea pig histamine H1-receptor. Mol Pharmacol 2009;76:25–37.
52. Tanford C. The hydrophobic effect. New York, NY, John Wiley: 1980.
53. Strajbl M, Florian J, Warshel A. Ab initio evaluation of the free energy surfaces for the general base/acid catalyzed thiolysis of formamide and the hydrolysis of methyl thioformate: a reference solution reaction for studies of cysteine proteases. J Phys Chem B 2001;105:4471–84.
54. Galesa K, Bren U, Kranjc A, Mavri J. Carcinogenicity of acrylamide: a computational study. J Agric Food Chem 2008;56:8720–7.
55. Allen PM, Tildesley DJ. Computer simulation of liquids. Oxford, Oxford University Press: 1987.
56. Van Gunsteren WF, Beredsen HJ. Computer simulation of molecular dynamics: methodology, applications and perspectives in chemistry. Angew Chem Int Ed Engl 1990;29:992–1023.
57. Jeziorski B, Kolos W. Perturbation approach to the study of weak intermolecular interactions. In: Ratajczak H, Orville-Thomas WJ, editors. Molecular interactions. Vol. 3. New York, NY, John Wiley: 1982:1–46.
58. Hirschfelder JO. Perturbation theory for exchange forces, I. Chem Phys Lett 1967;1:325–9.
59. Hirschfelder JO. Perturbation theory for exchange forces, II. Chem Phys Lett 1967;1:363–8.
60. Stone AJ. The theory of intermolecular forces. Oxford, Oxford University Press: 1997.
61. Murrell JN, Show G. Intermolecular forces in the region of small orbital overlap. J Chem Phys 1967;46:1768–72.
62. Musher JI, Amos AT. Theory of weak atomic and molecular interactions. Phys Rev 1967;164:31–43.
63. Certain PR, Hirschfelder JO, Kolos W, Wolniewicz L. Exchange and coulomb energy of H_2 determined by various perturbation methods. J Chem Phys 1968;49:24–35.
64. Le Fèvre RJ. Empirical calculations using atomic radius. A review. Adv Phys Org Chem 1965;3:1–12.
65. Bowen JP, Allinger NL. Molecular mechanics: the art and science of parameterization. In: Lipkowitz KB, Boyd DB, editors.), Reviews in computational chemistry, Vol. 2, New York, NY, VCH Publishers: 1991:81–97.
66. Schlick T. Molecular modeling and simulation: an interdisciplinary guide interdisciplinary applied mathematics: mathematical: biology. New York, NY, Springer-Verlag: 2000.
67. van Duin AC, Dasgupta S, Lorant F, Goddard WA, Reax. FF: A reactive force field for hydrocarbons. J Phys Chem A 2001;105:9396–409.
68. Verlet L. Computer 'experiments' on classical fluids. I. Thermodynamical properties of Lennard-Jones molecules. Phys Rev 1967;159:98–103.
69. Hirst DM. A computational approach to chemistry. Oxford, Blackwell: 1990.
70. Metropolis N, Rosenbluth AW, Rosenbluth MN, Teller AH, Teller E. Equation of state calculations by fast computing machines. J Chem Phys 1953;21:1087–92.
71. Adams DJ. Introduction to Monte Carlo simulation techniques. In: Perran JW, editors. Physics of superionic conductors and electrode materials. New York, NY, Plenum: 1983:177–95.
72. Zwanzig RW. High-temperature equation of state by a perturbation method. I. Nonpolar gases. J Chem Phys 1954;22:1420–6.
73. Martinek V, Bren U, Goodman MF, Warshel A, Florian J. DNA polymerase β catalytic efficiency mirrors the Asn279-dCTP H-bonding strength. FEBS Lett 2007;581:775–80.
74. Udommaneethanakit T, Rungrotmongkol T, Bren U, Frecer V, Miertus S. Dynamic behavior of avian influenza A virus neuraminidase subtype H5N1 in complex with oseltamivir, zanamivir, peramivir, and their phosphonate analogues. J Chem Inf Model 2009;49:2323–32.
75. Knight JL, Brooks CL, 3rd. Lambda-dynamics free energy simulation methods. J Comput Chem 2009;30:1692–700.
76. Kästner J, Senn HM, Thiel S, Otte N, Thiel W. QM/MM free-energy perturbation compared to thermodynamic integration and umbrella sampling: application to an enzymatic reaction. J Chem Theory Comput 2006;2:452–61.
77. Steiner D, Oostenbrink C, Diederich F, Zürcher M, van Gunsteren WF. Calculation of binding free energies of inhibitors to plasmepsin II. J Comput Chem 2011;32:1801–12.
78. Genheden S, Nilsson I, Ryde U. Binding affinities of factor Xa inhibitors estimated by thermodynamic integration and MM/GBSA. J Chem Inf Model 2011;51:947–58.
79. Bren U, Martinek V, Florian J. Decomposition of the solvation free energies of deoxyribonucleoside triphosphates using the free energy perturbation method. J Phys Chem B 2006;110:12782–8.
80. Warshel A, Levitt M. Theoretical studies of enzymic reactions: dielectric, electrostatic and steric stabilization of the carbonium ion in the reaction of lysozyme. J Mol Biol 1976;103:227–49.
81. Singh UC, Kollman PA. A combined ab initio quantum-mechanical and molecular mechanical method for carrying out simulations on complex molecular systems. Applications to the CH_3Cl+Cl^- exchange reaction and gas-phase protonation of polyethers. J Comput Chem 1986;7:718–30.
82. Field MJ, Bash PA, Karplus M. Combined quantum-mechanical and molecular mechanical potential for molecular dynamics simulations. J Comput Chem 1990;11:700–33.
83. Svensson M, Humbel S, Morokuma J. Energetics using the single point IMOMO (integrated molecular orbital+molecular orbital) calculations: choices of computational levels and model system. J Chem Phys 1996;105:3654–61.
84. Svensson M, Humbel S, Froese RD, Matsubara T, Siebe S, Morokuma J. ONIOM: a multilayered integrated MO+MM method for geometry optimizations and single point energy predictions. J Phys Chem 1996;100:19357–63.
85. Frisch MJ, Trucks GW, Schlegel HB, Scuseria GE, Robb MA, Cheeseman JR, et al. Gaussian 09. Wallingford, CT, Gaussian, Inc., 2009.

86. Remko M, Lyne PD, Richards WG. Molecular structure, gas-phase acidity and basicity of N-hydroxyurea. Phys Chem Chem Phys 2000;2:2511–4.
87. Senn H, Thiel W. QM/MM studies of enzymes. Curr Opin Chem Biol 2007;11:182–7.
88. Srinivasan J, Cheatham TE, Cieplak P, Kollman PA, Case DA. Continuum solvent studies of the stability of DNA, RNA, and phosphoramidate-DNA helices. J Am Chem Soc 1998;120:9401–9.
89. Massova I, Kollman PA. Computational alanine scanning to probe protein–protein interactions: a novel approach to evaluate binding free energies. J Am Chem Soc 1999;121:8133–43.
90. Sitkoff D, Sharp KA, Honig B. Accurate calculation of hydration free energies using macroscopic continuum models. J Phys Chem 1998;98:1978–83.
91. Kollman PA, Massova I, Reyes C, Kuhn B, Huo S, Chong L, et al. Calculating structures and free energies of complex molecules: combining molecular mechanics and continuum models. Acc Chem Res 2000;33:889–97.
92. Foloppe N, Hubbard R. Towards predictive ligand design with free-energy based computational methods? Curr Med Chem 2006;13:3583–608.
93. Åqvist J, Medina C, Samuelsson J-E. A new method for predicting binding affinity in computer-aided drug design. Protein Eng 1994;7:385–91.
94. Hansson T, Marelius J, Åqvist J. Ligand binding affinity prediction by linear interaction energy methods. J Comput-Aided Mol Des 1998;12:27–35.
95. Almlöf M, Brandsdal BO, Åqvist J. Binding affinity prediction with different force fields: examination of the linear interaction energy method. J Comput Chem 2004;25:1242–54.
96. Almlöf M, Carlsson J, Åqvist J. Improving the accuracy of the linear interaction energy method for solvation free energies. J Chem Theory Comp 2007;3:2162–75.
97. de Amorim HL, Caceres RA, Netz PA. Linear interaction energy (LIE) method in lead discovery and optimization. Curr Drug Targets 2008;9:1100–5.
98. Ersmark K, Nervall M, Hamelink E, Janka LK, Clemente JC, Dunn BM, et al. Synthesis of malarial plasmepsin inhibitors and prediction of binding modes by molecular dynamics simulations. J Med Chem 2005;48:6090–106.
99. Bjelic S, Nervall M, Gutiérrez-de-Terán H, Ersmark K, Hallberg A, Åqvist J. Computational inhibitor design against malaria plasmepsins. Cell Life Sci 2007;64:2285–305.
100. Lee FS, Chu Z-T, Bolger MB, Warshel A. Calculations of antibody-antigen interactions: microscopic and semi-microscopic evaluation of the free energies of binding of phosphorylcholine analogs to McPC603. Protein Eng 1992;5:215–28.
101. Frecer V, Miertus S, Tossi A, Romeo D. Rational design of inhibitors for drug-resistant HIV-1 aspartic protease mutants. Drug Des Disc 1998;15:211–31.
102. Miertus S, Frecer V, Majekova M. The extended polarizable continuum model of solvation for calculation of solvent effects. J Mol Struct (Theochem) 1988;179:353–66.
103. Frecer V, Majekova M, Miertus S. Approximate methods for the solvation of large biomolecules. J Mol Struct (Theochem) 1989;183:403–16.
104. Frecer V, Miertus S, Majekova M. Modelling of dispersion and repulsion interactions in liquids. J Mol Struct (Theochem) 1991;227:157–73.
105. Frecer V, Miertus S. Polarizable continuum model of solvation for biopolymers. Int J Quant Chem 1992;42:1449–68.
106. Miertus S, Frecer V. Continuum models of environmental effects on molecular structure and mechanisms in chemistry and biology. J Math Chem 1992;10:183–204.
107. Fischer S, Smith JC, Verma C. Dissecting the vibrational entropy change on protein/ligand binding: burial of a water molecule in bovine pancreatic trypsin inhibitor. J Phys Chem B 2001;105:8050–5.
108. Frecer V, Miertus S. Interactions of ligands with macromolecules: rational design of specific inhibitors of aspartic protease of HIV-1. Macromol Chem Phys 2002;203: 1650–7.
109. Frecer V, Kabelac M, De Nardi P, Pricl S, Miertus S. Design of inhibitors of hepatitis C virus NS3 serine protease. J Mol Graphics Modell 2004;22:209–20.
110. Frecer V, Berti F, Benedetti F, Miertus S. Design of peptidomimetic inhibitors of aspartic protease of HIV-1 including –PheΨPro– core and favorable ADME properties. J Mol Graphics Modell 2008;27:376–87.
111. Frecer V, Seneci P, Miertus S. Computer-assisted combinatorial design of bicyclic thymidine analogs as inhibitors of mycobacterium tuberculosis thymidine monophosphate kinase. J Comp-Aided Mol Des 2011;25:31–49.
112. Taylor RD, Jewsbury PJ, Essex JW. A review of protein small molecule docking methods. J Comput Aided Mol Des 2002;16:151–66.
113. Klebe G. Virtual ligand screening: strategies, perspectives and limitations. Drug Discov Today 2006;11:580–94.
114. Kitchen DB, Decornez H, Furr JR, Bajorath J. Docking and scoring in virtual screening of drug discovery: methods and applications. Nat Rev Drug Discov 2004;3:935–49.
115. Moitessier N, Englebienne P, Lee D, Lawandi J, Corbeil CR. Towards the development of universal, fast and highly accurate docking/scoring methods: a long way to go. Br J Pharmacol 2008:153:S7–S26.
116. Bissantz C, Folkers G, Rognan D. Protein-based virtual screening of chemical databases. 1. Evaluation of different docking/scoring combinations. J Med Chem 2000;43:4759–67.
117. Englebienne P, Fiaux H, Kuntz DA, Corbeil CR, Gerber-Lemaire S, Rose DR, et al. Evaluation of docking programs for predicting binding of Golgi alpha-mannosidase ii inhibitors: a comparison with crystallography. Proteins Struct Funct Bioinf 2007;69:160–76.
118. Warren GL, Andrews CW, Capelli AM, Clarke B, LaLonde J, Lambert MH, et al. A critical assessment of docking programs and scoring functions. J Med Chem 2006;49: 5912–31.